Bioorganic & Medicinal Chemistry Letters 20 (2010) 5510–5513

Contents lists available at ScienceDirect

Bioorganic & Medicinal Chemistry Letters

journal homepage: www.elsevier.com/locate/bmcl

Relationships between structures of hydroxyflavones and their antioxidative effects

Jiye Hyun [a], Yoonkyung Woo [a], Do-seok Hwang [a], Geunhyeong Jo [a], Sunglock Eom [a], Younggiu Lee [a], Jun Cheol Park [b], Yoongho Lim [a,*]

[a] Division of Bioscience and Biotechnology, BMIC, RCD, Konkuk University, Seoul 143-701, Republic of Korea
[b] National Institute of Animal Science, Rural Development Administration, Suwon 441-706, Republic of Korea

ARTICLE INFO

Article history:
Received 18 May 2010
Revised 13 July 2010
Accepted 16 July 2010
Available online 21 July 2010

Keywords:
Flavone
Antioxidative effects
QSAR

ABSTRACT

Even hydroxyflavones show diverse biological functions, they have two common features such as showing antioxidative effects and containing hydroxyl groups. The authors tested the antioxidative effects of thirty hydroxyflavones using 1,1-diphenyl-2-picrylhydrazyl radical scavenging assay. While the scavenging activity of galangin, 3,5,7-trihydroxyflavone was 52.5%, fisetin, 3,7,3′,4′-tetrahydroxyflavone showed 85.2%. To investigate the relationships between the structures of hydroxyflavones and their antioxidative effects, the three-dimensional quantitative structure–activity relationships were examined.

Flavonoids are found ubiquitously in plants as secondary metabolites and according to the International Union of Pure and Applied Chemistry (IUPAC) nomenclature they can be classified to flavonoids, isoflavonoids, and neoflavonoids which have moieties such as 2-phenylchromen-4-one, 3-phenylchromen-4-one, and 4-phenylcoumarin, respectively. They show diverse biological functions. A pentahydroxyflavonoid, quercetin shows anti-inflammatory effect in airway allergic inflammatory mice model,[1] another pentahydroxyflavonoid, morin regulates the expression of nuclear factor kappa-light-chain-enhancer of activated B cells,[2] hexahydroxyflavonoid, quercetagetin inhibits tomato bushy stunt virus infection,[3] another hexahydroxyflavonoid, myricetin is known to inhibit cell transformation,[4] and tetrahydroxyflavonoid, kaempferol inhibits angiogenesis.[5] These hydroxyflavonoids have two common features: they show antioxidative effects and belong to flavones. Flavonoids consist of C6–C3–C6 skeleton. In flavones, this skeleton is composed of three rings, A-, C-, and B-ring, respectively. It is known that many flavones show antioxidative effects. The authors tested the antioxidative effects of 30 hydroxyflavones using 1,1-diphenyl-2-picrylhydrazyl (DPPH) radical scavenging assay. While the scavenging activity of galangin, 3,5,7-trihydroxyflavone was 52.5%, fisetin, 3,7,3′,4′-tetrahydroxyflavone showed 85.2%. They have 3-hydroxychrome-4-one moiety, but the number of hydroxyl groups and their positions are different. Here, the activity was compared to vitamin C of 89.1% and vitamin E of 59.9%. The test compounds include three dihydroxyflavones, nine trihydroxyflavones, 11 tetrahydroxyflavones, five pentahydroxyflavones, and two hexahydroxyflavones. Because simple intuitional analysis cannot explain this phenomenon, a computational analysis, three-dimensional quantitative structure–activity relationships (3D-QSAR) was applied.

In order to elucidate the relationships between the structures of hydroxyflavones and their antioxidative effects, the DPPH radical scavenging assay was first carried out.[6] All flavone derivatives were purchased from Indofine Chemical Co. Inc. (Hillsborough, NJ). The 3D-QSAR calculations were examined using the SYBYL 7.3 program.[7] The 30 compounds were divided into two groups: a training set of 24 compounds to create QSAR models, and a test set of six compounds (**4**, **8**, **12**, **17**, **18**, and **29** in Table 1) to validate the models. The structures of the 30 hydroxyflavones and their antioxidative effects are given in Table 1.

Computational methods were carried out on a Linux PC workstation.[8,9] As mentioned above, flavonoids consist of a C6–C3–C6 skeleton which are named A-, C-, and B-rings, respectively. Because flavones do not include any chiral center, the 3D structures of the compounds used here were built up using SYBYL program based on the 3D structure of quercetin, 3,5,7,3′,4′-pentahydroxyflavone whose crystallographic structure can be obtained from the Protein Data Bank (2O3P pdb) where its crystal structure was deposited as an inhibitor for pim-1 kinase.[10] The initial structures of all hydroxyflavones were subjected to energy minimization.[11]

All compounds were aligned using the DATABASE Alignment module in the SYBYL program.[12] Compound **19**, 7,3′,4′,5′-tetrahydroxyflavone showing the best activity value, was used as a template and the atom-based root mean square (rms) fit method with

* Corresponding author.
E-mail address: yoongho@konkuk.ac.kr (Y. Lim).

0960-894X/$ - see front matter © 2010 Elsevier Ltd. All rights reserved.
doi:10.1016/j.bmcl.2010.07.068

Table 1
Structures of the 30 hydroxyflavones and their antioxidative effects

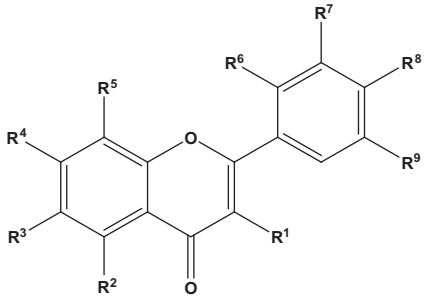

Training set	Nomenclature	R^1	R^2	R^3	R^4	R^5	R^6	R^7	R^8	R^9	Scavenging activity (%)
1	3,2′-Dihydroxyflavone	OH	H	H	H	H	OH	H	H	H	69.3
2	3,5,-Dihydroxyflavone	OH	OH	H	H	H	H	H	H	H	58.3
3	3′,5′-Dihydroxyflavone	H	H	H	H	H	H	OH	H	OH	61.8
5	3,5,7-Trihydroxyflavone (galangin)	OH	OH	H	OH	H	H	H	H	H	52.5
6	5,7,8-Trihydroxyflavone	H	OH	H	OH	OH	H	H	H	H	58.8
7	7,8,2′-Trihydroxyflavone	H	H	H	OH	OH	OH	H	H	H	79.9
9	6,2′,3′-Trihydroxyflavone	H	H	OH	H	H	OH	OH	H	H	87.1
10	6,3′,4′-Trihydroxyflavone	H	H	OH	H	H	H	OH	OH	H	83.9
11	7,3′,4′-Trihydroxyflavone	H	H	H	OH	H	H	OH	OH	H	84.9
13	3,7,3′,4′-Tetrahydroxyflavone (fisetin)	OH	H	H	OH	H	H	OH	OH	H	85.2
14	3,6,2′,3′-Tetrahydroxyflavone	OH	H	OH	H	H	OH	OH	H	H	86.6
15	3,6,3′,4′-Tetrahydroxyflavone	OH	H	OH	H	H	H	OH	OH	H	86.7
16	3,6,2′,4′-Tetrahydroxyflavone	OH	H	OH	H	H	OH	H	OH	H	86.3
19	7,3′,4′,5′-Tetrahydroxyflavone	H	H	H	OH	H	H	OH	OH	OH	88.8
20	5,6,7,4′-Tetrahydroxyflavone (6-hydroxyapigenin)	H	OH	OH	OH	H	H	H	OH	H	69.9
21	7,8,3′,4′-Tetrahydroxyflavone	H	H	H	OH	OH	H	OH	OH	H	87.4
22	3,7,8,2′-Tetrahydroxyflavone	OH	H	H	OH	OH	OH	H	H	H	83.1
23	6,7,3′,4′-Tetrahydroxyflavone	H	H	OH	OH	H	H	OH	OH	H	86.4
24	3,5,7,2′,4′-Pentahydroxyflavone (morin)	OH	OH	H	OH	H	OH	H	OH	H	81.5
25	3,5,7,3′,4′-Pentahydroxyflavone (quercetin dehydrate)	OH	OH	H	OH	H	H	OH	OH	H	87.8
26	5,7,3′,4′,5′-Pentahydroxyflavone	H	OH	H	OH	H	H	OH	OH	OH	88.1
27	3,6,2′,4′,5′-Pentahydroxyflavone	OH	H	OH	H	H	OH	H	OH	OH	85.6
28	3,7,3′,4′,5′-Pentahydroxyflavone	OH	H	H	OH	H	H	OH	OH	OH	79.9
30	3,5,7,8,3′,4′-Hexahydroxyflavone (gossypetin)	OH	OH	H	OH	OH	H	OH	OH	H	85.4
Test set											
4	3,3′,4′-Trihydroxyflavone	OH	H	H	H	H	H	OH	OH	H	85.7
8	7,8,3′-Trihydroxyflavone	H	H	H	OH	OH	H	OH	H	H	87.1
12	3,6,2′-Trihydroxyflavone	OH	H	OH	H	H	OH	H	H	H	86.8
17	3,5,7,2′-Tetrahydroxyflavone (datiscetin)	OH	OH	H	OH	H	OH	H	H	H	86.5
18	3,5,7,4′-Tetrahydroxyflavone (kaempferol)	OH	OH	H	OH	H	H	H	OH	H	77.2
29	3,5,7,3′,4′,5′-Hexahydroxyflavone (myricetin)	OH	OH	H	OH	H	H	OH	OH	OH	79.5

DATABASE ALIGN option in SYBYL was adapted.[13] A training set was used for comparative molecular field analysis (CoMFA). The steric and electrostatic field energies were calculated using Lennard–Jones 6–12 potential and Coulombic potential, respectively.[14] Since comparative molecular similarity indices analysis (CoMSIA) can calculate the steric and electrostatic fields as well as the hydrophobic, hydrogen bond (H-bond) donor, and H-bond acceptor fields, the contour maps obtained from CoMSIA were useful. The partial least square (PLS) analysis was carried out to examine the correlation between the biological activities and descriptors showing the physicochemical properties of the compounds. The cross-validation analysis was performed using the 'leave one out' (LOO) method. The optimum number of components obtained from the LOO method was applied to derive the final non-cross-validated correlation r^2. The best CoMFA or CoMSIA model was improved by a region focusing method.

Among the several models generated from CoMFA, the model showing the best cross-validated value (q^2 = 0.888) was chosen. In this experiment, the r^2 value was 0.978. The number of components and standard error of estimate were 6 and 1.919, respectively. *F* value for PLS was 125.311. The best CoMFA model was obtained with a region focusing method. To check the CoMFA model, the activities of the compounds contained in the training set were

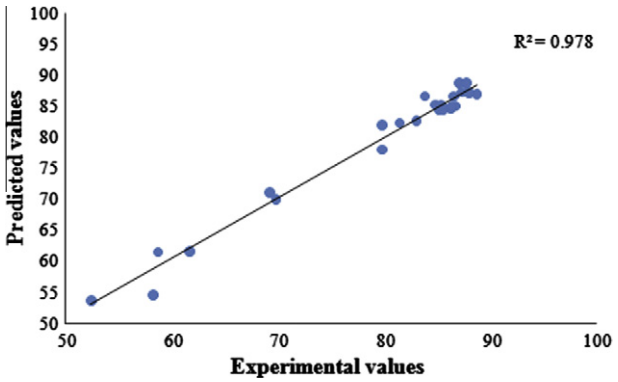

Figure 1. Correlation between experimental and predicted values from the CoMFA model.

predicted and compared to the experimental data (Fig. 1). The residual values between the experimental and predicted values for the training set ranged within 6%.[13] The maximum residual value was observed in 3,5-dihydroxyflavone whose experimental scavenging effect was 58.3% and calculated value, 54.6%. To validate the QSAR model, a test set was selected. The residual values between the experimental and predicted values for the test set were less than 19%.[13] The largest residual value was observed in datiscetin. Therefore, the CoMFA model was good for the test set.

As mentioned above, to calculate the steric and electrostatic fields as well as the hydrophobic, H-bond donor, and H-bond acceptor fields, the several models of CoMSIA were generated. Of them, the model displaying the best cross-validated value ($q^2 = 0.770$) was selected. The corresponding r^2 was 0.947.[13] The number of components and standard error of estimate were 6 and 2.975, respectively. *F* value for PLS was 50.504. The residual values between the experimental and predicted values for the training set ranged from 7%.[13] The largest residual value was observed in galangin and 3,7,8,2′-tetrahydroxyflavone. The residual values between the experimental and predicted values for the test set were less than 17%.[13] The maximum residual values was observed in 3,6,2′-trihydroxyflavone and datiscetin. The ranges of residuals obtained from the experimental and predicted values were small enough to be accepted.

To visualize the relationships between the structures and their activities, CoMFA contour maps were generated using SYBYL 7.3. The steric and electrostatic contributions are 32.9% and 67.1%, respectively, and are depicted in Figure 2. In the electrostatic field, the electronegative favored region contributed 74% and the electropositive favored region 26%. The electronegative region colored in red contained the 4-position of the C-ring and the 7-position of the A-ring. In the case of the steric field, the steric bulky favored region contributed 15% and the disfavored region 85%. The bulky favored region contained the 3′,4′,5′-positions of the B-ring and 7-position of the A-ring.

In order to obtain information on the steric, electrostatic, hydrophobic, and hydrogen bond (H-bond) donor properties, CoMSIA contour maps were generated (Fig. 3). Their fields were contributed as 1.7%, 40.7%, 9.5%, and 48.1%, respectively. In the case of the steric field, the steric bulky favored region contributed 6% and the disfavored region 94%. The bulky favored region contained 3′-position of the B-ring and 4-position of the C-ring; the bulky disfavored region, 6′-pisition of the B-ring. In the electrostatic field, the electronegative favored region contributed 85% and the electropositive favored region 15%. The electronegative region was near 3′-position of the B-ring. The hydrophobic contour map

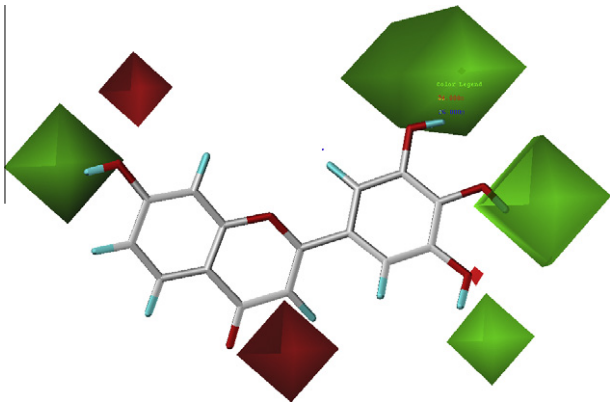

Figure 2. CoMFA contour maps. The corresponding steric and electrostatic field contributions are 32.9% and 67.1%, respectively. The electrostatic field contours are shown in red (electronegative substituent favored), while the steric field contours are shown in green (more bulk favored).

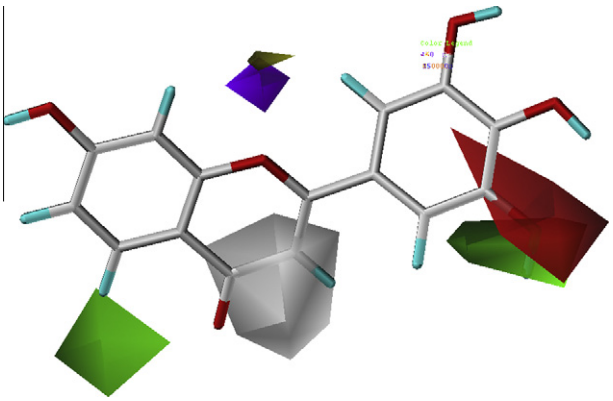

Figure 3. More bulk favored (green), electronegative favored (red), hydrophilic favored (white), and H-bond donor disfavored (purple) region contours are shown in CoMSIA contour maps. The corresponding field contributions of steric, electrostatic, hydrophobic, and H-bond donor are 1.7%, 40.7%, 9.5%, and 48.1%, respectively.

indicates the hydrophobic substituent favored region and the hydrophilic substituent favored region which were contributed as 8% and 92%, respectively. The hydrophilic region was near the 4-position of the B-ring. The H-bond donor favored region and disfavored region were contributed as 96% and 4%, respectively. The disfavored region was observed between the 8-position of the A-ring and the 6′-position of the B-ring.

As a result, the structural conditions of hydroxyflavone to show the good scavenging effect are as follows: As the number of hydroxyl groups increases, the derivatives have a tendency to show better scavenging effects. In addition, two hydroxyl groups neighboring to each other show better effects too. For example, 3,5,7-trihydroxyflavone shows the activity of 52.5% which is lower than that of dihydroxyflavones. When the 3′-position has the bulky group, according to the CoMFA results the derivative shows better activity such as 6,2′,3′-trihydroxyflavone and 7,8,3′-trihydroxyflavone. The same phenomenon was observed in the results obtained by the authors previously.[15] The scavenging effects of four trihydroxyflavones, 5,7,2′-trihydroxyflavone, 5,3′,4′-trihydroxyflavone, 6,7,3′-trihydroxyflavone, and 7,8,4′-trihydroxyflavone were measured and their activities were 9.7%, 81.0%, 87.8%, and 87.7%, respectively. Even though they all contain three hydroxyl groups, compounds with hydroxyl groups neighboring to each other showed much higher antioxidative activities than the compound with separated hydroxyl groups. In the case of dihydroxyflavone, the same result was observed.[16] While 2′,3′-dihydroxyflavone showed 85.8%, 2′,4′-dihydroxyflavone did 40.4%. Therefore, *ortho* position of dihydroxyl groups is one of the structural conditions of hydroxyflavone for the good scavenging effect.

Acknowledgments

This work was supported by Priority Research Centers Program through the National Research Foundation of Korea funded by the Ministry of Education, Science and Technology (2009-0093824), the Korean Rural Development Administration (Biogreen21 Program, 20080401034052), Agenda Program (NIAS, 11-30-68), and Disease Network Research Program Grant (NRF, M10751050004-07N5105-00410).

Supplementary data

Supplementary data associated with this article can be found, in the online version, at doi:10.1016/j.bmcl.2010.07.068.

References and notes

1. Rogerio, A. P.; Dora, C. L.; Andrade, E. L.; Chaves, J. S.; Silva, L. F.; Lemos-Senna, E.; Calixto, J. B. *Pharmacol. Res.* **2010**, *61*, 288.
2. Sivaramakrishnan, V.; Niranjali Devaraj, S. *Chem. Biol. Interact.* **2009**, *180*, 353.
3. Rusak, G.; Krajaci, M.; Plese, N. *Antiviral Res.* **1997**, *36*, 125.
4. Kumamoto, T.; Fujii, M.; Hou, D. X. *Mol. Cell. Biochem.* **2009**, *332*, 33.
5. Luo, H.; Rankin, G. O.; Liu, L.; Daddysman, M. K.; Jiang, B. H.; Chen, Y. C. *Nutr. Cancer* **2009**, *61*, 554.
6. The samples were dissolved in 0.1% aqueous methanol. One millilitre of 100 mM Tris–HCl buffer (pH 7.4) was added into 100 μL sample solution. The solution of DPPH radicals was prepared in 1 mL of a 0.5 mM aqueous methanol. The mixture of the sample solution and DPPH solution was left during 15 min at 37 °C and its absorbance was measured with a spectrophotometer (Shimadzu, Tokyo, Japan) at 517 nm. The %scavenging effects were calculated using the equation: [1 − (absorbance of sample/absorbance of control)] × 100.
7. Kim, H.; Lee, E.; Kim, J.; Jung, B.; Chong, Y.; Ahn, J. H.; Lim, Y. *Bioorg. Med. Chem. Lett.* **2008**, *18*, 661.
8. Lee, S.; Woo, Y.; Shin, S. Y.; Lee, Y. H.; Lim, Y. *Bioorg. Med. Chem. Lett.* **2009**, *19*, 2116.
9. The structures used in this experiment were subjected to energy minimization. All calculations were performed on an Intel Core 2 Quad Q6600 (2.4 GHz) Linux PC with SYBYL 7.3 (Tripos, St. Louis, MO).[14]
10. Holder, S.; Zemskova, M.; Zhang, C.; Tabrizizad, M.; Bremer, R.; Neidigh, J. W.; Lilly, MB. *Mol. Cancer Ther.* **2007**, *6*, 163.
11. The energy minimization process was stopped when the total energy reached 0.05 kcal/mol Å.
12. The aligned molecules were put into in a three dimensional cubic lattice whose size was 2.0 Å × 2.0 Å × 2.0 Å.
13. Data not shown in the text can be found in Supplementary data.
14. Klebe, G.; Abraham, U.; Mietzner, T. *J. Med. Chem.* **1994**, *37*, 4130.
15. Park, Y.; Lee, S.; Woo, Y.; Lim, Y. *Bull. Korean Chem. Soc.* **2009**, *30*, 1397.
16. Young, J. M.; Park, Y. H.; Lee, Y. U.; Kim, H. J.; Shim, Y. H.; Ahn, J. H.; Lim, Y. H. *J. Microbiol. Biotechnol.* **2007**, *17*, 530.